Research Square

Preprints are preliminary reports that have not undergone peer review.
They should not be considered conclusive, used to inform clinical practice,
or referenced by the media as validated information.

The Tsunami Source Generated by the July 29, 2025 Kamchatka Earthquake Reconstructed as a Solution of the Inverse Problem

Tatyana A. Voronina

tanvor@bk.ru

The Institute of Computational Mathematics and Mathematical Geophysics SB RAS

Vladislav V. Voronin

Novosibirsk State University

Maxim A. Gorodnichev

The Institute of Computational Mathematics and Mathematical Geophysics SB RAS

Research Article

Keywords: tsunami, numerical modeling, inverse ill-posed problem, singular value decomposition, specific energy

Posted Date: June 22nd, 2026

DOI: https://doi.org/10.21203/rs.3.rs-9912422/v1

License: This work is licensed under a Creative Commons Attribution 4.0 International License.
Read Full License

Additional Declarations: No competing interests reported.

The Tsunami Source Generated by the July 29, 2025 Kamchatka Earthquake Reconstructed as a Solution of the Inverse Problem

Tatyana A. Voronina [1], Vladislav V. Voronin [2], Maxim A. Gorodnichev [1,2,3]
[1] The Institute of Computational Mathematics and Mathematical Geophysics SB RAS,
Pr. Ac. Lavrentieva, 6, Novosibirsk 630090, Russia
tanvor@bk.ru
[2]Novosibirsk State University,
Pirogova Str., Novosibirsk, 630090, Russia
[3]Novosibirsk State Technical University
Prospekt K. Marksa, 20, Novosibirsk, 630073, Russia

Abstract. We propose a source model for the tsunamigenic earthquake of July 29, 2025 (Mw 8.8) off the coast of Kamchatka based on the inversion of remote tsunami waveforms. The truncated singular value decomposition method (SVD, or r-solution method) was used for the tsunami waveform inversion. This approach significantly reduces the numerical instability caused by the ill-posedness of the problem and successfully recovers the initial sea surface displacement in the tsunami source area. Furthermore, the method allows us to compute tsunami waveforms at a priori selected locations of interest, even when no observational data are available at those locations. The latter is made possible by selecting the so-called "most informative" data according to the methodology proposed in this paper.

Keywords: tsunami, numerical modeling, inverse ill-posed problem, singular value decomposition, specific energy

Acknowledgments: This study was supported by the Ministry of Science and Higher Education of the Russian Federation through the Institute of Computational Mathematics and Mathematical Geophysics of the Siberian Branch of the Russian Academy of Sciences (State Assignment 2025, Topics FWNM-2025-0004, FWNM-2025-0005). The authors express their gratitude to A.V. Lander, Senior Researcher at the Institute of Earthquake Prediction Theory and Mathematical Geophysics of the Russian Academy of Sciences, for providing the processed observation data.

1 Introduction

The Tsunami Warning System (TWS) is designed to provide timely warning of a tsunami hazard. A significant part of tsunami forecasting is knowing the initial tsunami waveform (below referred to as the tsunami source), which is especially important in near-shore zones, where the impact of a tsunami wave is largely dependent on the source geometry (Okal & Synolakis, 2004). The lack of any direct observations at the moment of an earthquake in the tsunami source area makes the reconstruction of the initial water displacement by inverting remote sea-level records an important tool in the Tsunami Warning System. It is well known that the above problem is an ill-posed one, furthermore, the observed sea-level records are very noisy. The most well-known method for solving this inverse problem is numerical modeling. For the reasons stated above, obtaining a stable numerical solution is challenging. The latter imposes severe constraints on both the mathematical methods employed and the observational system (An, 2020).

The unknown tsunami source function is typically approximated by a linear combination of basis functions in an a priori defined domain. The unknown coefficients of this decomposition are determined as a solution to a minimization problem with an appropriate choice of a functional (which, in a broad sense, also includes the type of observed data). Since the problem is ill-posed, different solutions can often reproduce the observed data (within the assumed noise level). Therefore, the minimized functional always includes a regularization term, which can be viewed as introducing a priori assumptions to select a physically justified and robust solution.

Sometimes, instead of adding a regularizing term to the functional, a truncated singular value decomposition (SVD) method is used, which stabilizes the solution by discarding small singular values (Cheverda & Kostin, 2010; Voronina, 2011). Regularization often underestimates the source amplitude. In modern studies (e.g., Takagawa et al., 2025), correction methods are being developed to preserve the physical accuracy of wave heights without losing the stability of the inversion. Various options exist for constructing the functional and selecting basis functions.

A well-known choice for the basis functions is the so-called Green's functions, first introduced by Satake (1987) to represent the tsunami source function in the inversion of tsunami waveforms. The linear inversion method has become a classic approach for subsequent tsunami studies (e.g., Mulia et al., 2018; Piatanesi et al., 2001). Another option employed at NOAA PMEL (National Oceanic and Atmospheric Administration Pacific Marine

Environmental Laboratory) to represent the tsunami source is to use a decomposition with a set of special model sources of a simple form with unknown coefficients. This approach has been successfully applied in the "minimum residual" method (Percival, 2011) to reconstruct the tsunami source for several real events. While most research papers focus on linear inversion methods, accounting for the nonlinear nature of tsunami waveforms may be significant for assessing tsunami inundation (Satake, 1995; Baba et al., 2015; Romano et al., 2016). One of the widely used nonlinear methods is the adjoint method, introduced to the tsunami community by Pires & Miranda (2001) to solve minimization problems of large nonlinear systems that always present in above problem (e.g., Mulia et al., 2018; Hossen et al., 2018).

Using inversion methods for tsunami source reconstruction in real-world cases has led to the understanding that the spatial arrangement of monitoring sensors relative to the source region has a greater impact on inversion results than their number. The optimal placement of tsunami sensors has been the subject of numerous studies (An et al., 2018; Lee et al., 2019; Mulia et al., 2017, 2018; Meza et al., 2018; Voronina & Voronin, 2023, 2025). It has been established that the optimal location of stations is closely related to the directions of the most intense tsunami energy propagation. These directions are believed to correlate with the "most complete information content" of the passing wave.

Since full numerical modeling is often prohibitively expensive in terms of computations and time, recent research suggests that there is an alternative that makes use of machine learning. These methods (sometimes using neural networks) are beginning to be used in tsunami modeling, as they can help automate and improve the accuracy of source reconstruction (Mulia et al., 2016, 2020; Song et al., 2023). A recent and comprehensive review of tsunami inversion methods, including machine learning techniques, can be found in Gusman & Tanioka (2022). A further advance in solving the problem under consideration is streaming data assimilation, a more general and promising approach than pure inversion (Wang, 2019). Instead of searching for a single "best" solution, data assimilation methods continually adjust the model as new data arrive in real time. This is a direct evolutionary step from minimization problems.

In this paper, the inversion is performed using remote measurements of deep water-level data produced by DART (Deep-ocean Assessment and Reporting of Tsunamis) buoys as the observation data. Tsunami wave propagation (the forward problem) is described by the linear theory of wave propagation and is discretized with the help of a finite-difference approach. The tsunami source is represented as a truncated Fourier series of spatial harmonics with unknown coefficients (Cheverda & Kostin, 2010; Voronina et al., 2015). These unknown coefficients are determined by the least squares method with the truncated singular value decomposition (SVD) method as regularization. More specifically, the regularization is performed by restricting the operator to a subspace that is the linear hull of the first ***r*** right-hand singular vectors. The dimensionality of the subspace depends on the observation system, bathymetry, and noise (Voronina, 2016). One of the advantages of the proposed method is the opportunity to compute tsunami waveforms at any predetermined points (in cases where observation data are missing at those points) without recalculating tsunami wave propagation using the reconstructed tsunami source. Based on the analysis of the distribution of the specific energy at the monitoring sensor locations, a method is proposed to select the most informative set of sensors for a given observation system. As it turned out, the best arrangement of the recorders is tightly correlated with the directions of the most intensive propagation of the tsunami energy (Voronina & Voronin, 2023).

Section 1 — Introduction. **Section 2** — Statement of the problem. **Section 3** — A brief description of the method. **Section 4** — Definition of the dimension of the solution subspace (parameter r). **Section 5** — Selection of the most informative data. **Section 6** — An example of tsunami source reconstruction using the most informative part of the observation system. **Section 7** — Examples of the reconstruction of waveform amplitudes at "predicted points" where there were no observations. **Section 8** — Conclusion. **Section 9** — References.

2 Model and Data

It is assumed that: (1) the tsunami wave is generated by a sharp rise and fall of the seafloor at an initial point in time, prior to which everything was at rest; (2) the water surface follows the shape of the seafloor movement at the tsunami source; (3) the linear approximation of "shallow" water can be used to describe the tsunami wave propagation process for the entire region, from the generation zone to the locations of deep-sea free surface level sensors; (4) the conditions of total reflection at solid boundaries and the conditions of wave permeability at the boundaries of the open sea are established; (5) the geography of the tsunami source region $\Omega(x, y)$ is assumed to be known from seismic data. The curvature of the Earth is neglected, which is typical when studying regional tsunamis. The problem is considered in a Cartesian coordinate system, where the z-axis is aligned with the direction of gravity. The modeling domain covers the area between 148°E–179°E and 38°N–55°N (Fig1). A 1-arc-minute grid was used to calculate tsunami propagation. Bathymetry data for the grid were obtained from the publicly available GEBCO_09 grid (version 20091120, http://www.gebco.net).

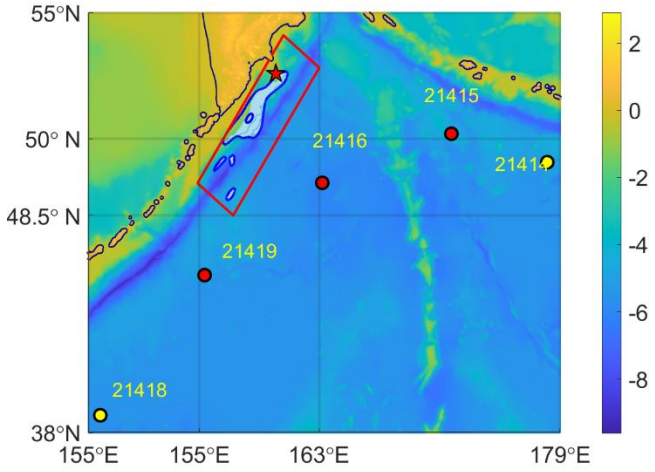


Fig. 1 The simulation domain of the Kamchatka Tsunami of July 29, 2025. The red rectangle marks the target domain; the red star marks the earthquake epicenter; the DART buoys are enumerated clockwise and marked by small circles: 1 – 21418, 2 – 21419, 3 – 21416, 4 – 21415, 5 – 21414; the dark blue lines correspond to the zero depth; the area bounded by the dark blue line inside the red rectangle is the projection of the reconstructed source on the surface z=0

In Figure1, the DART buoys whose data were considered the most informative are marked with red circles; the white circles indicate locations that were used as forecast points in some numerical calculations (see Section 6, Fig. 5 particularly). The target domain had to be selected based on an analysis of the kinematic characteristics of the observed waves. As a result, the target domain takes the form of a rectangle rotated relative to the modeling domain grid (Fig. 1). In this rotated rectangle, the source function is represented as a sum of spatial harmonics with unknown coefficients. The wave propagation problem is approximated by using a finite-difference approach with an explicit-implicit difference scheme constructed on a four-point template and a uniform rectangular staggered grid. The scheme has a second-order approximation in spatial variables and a first-order approximation in time: $\Delta t = 2$ s; $\Delta x = 1.42$ km; $\Delta y = 1.85$ km. To avoid interference from ports or local shelf effects, the records of the deep-sea DART buoys with IDs 21418, 21419, 21416, 21415, and 21414 were used in the calculations. All recordings were pre-processed to remove tides and resample at 2-second intervals. The tsunami waveforms of the 2025 Kamchatka earthquake are available at the NOAA National Data Buoy Center (https://www.ndbc.noaa.gov/obs.shtml).

3 The Method

The approach used in this study has already been applied to reconstruct the sources of the tsunamis of February 6, 2013, in the Solomon Islands, the Illapel tsunami in Chile on November 16, 2015, and the Shikotan tsunami on October 5, 1994. The results obtained and full description of the method were published in previous papers (e.g., Voronina, 2016, Voronina et al, 2019, 2021).
Briefly, the objective function $\varphi\,(x, y)$, modeling the tsunami source in the target domain, is sought for as the solution of the inverse problem from the equation

$$\mathrm{W}\varphi(x, y,) = \boldsymbol{\eta}(t), \qquad (1)$$

where operator W is a compact linear operator that maps the initial water surface displacement $\varphi\,(x, y)$ to the data $\boldsymbol{\eta}(t)$,

$$\boldsymbol{\eta}(\,t) = \left(\eta(x_1, y_1, t), \eta(x_2, y_2, t), \dots, \eta\left(x_p, y_p, t\right)\right), \qquad M_i = (x_i, y_i), i = 1,2, \dots, P$$

i.e., to the waveforms recorded by the monitoring sensors in the set of points $\{M_i\}$. Hence, this operator equation of the first kind can be reduced to an infinite system of linear algebraic equations. The regularization is needed due to the ill-posedness of the problem.

The numerical solution implies the finite-dimensional approximation of the system obtained, the right side is also represented by a vector containing time samples. The unknown function $\varphi\,(x, y)$ is sought for as a finite Fourier series of spatial harmonics with unknown coefficients $\{c_{mn}\}$:

$$\varphi(x, y) = \sum_m^M \sum_n^N c_{mn}\, sin\frac{m\pi}{l_1}x\; sin\frac{n\pi}{l_2}y = \sum_m^M \sum_n^N c_{mn}\, \varphi_{mn}(x.y) \qquad (2)$$

To find these coefficients, the following system was obtained:

$$\mathbf{A_0 c} = \boldsymbol{\eta_0} \qquad (3)$$

The matrix $\mathbf{A_0}$: $(\mathrm{P} \times N_t) \times (M \times N)$ is the one whose columns consist of computed marigrams from all sensors for each spatial harmonic $\varphi_{mn}(x, y)$ as a source, $(x, y) \in [0, l_1] \times [0, l_2]$; $\vec{c}$ is a vector that contains coefficients $\{c_{mn}\}$ ordered in some way; $\boldsymbol{\eta_0}$ is the vector containing the observed tsunami waveforms.

Let's call this matrix $\mathbf{A_0}$ and this right-hand side *complete.*

Since the number of equations far exceeds the number of unknown coefficients, we are looking for a quasi-solution $\mathbf{c}^{[r]}$ rather than an exact solution.

We select for source recovery only the sensors that we consider to be the most informative.

In the columns of the complete matrix $\mathbf{A_0}$ we leave only the marigrams related to the selected sensors, and we do the same in the right part. We will denote the resulting matrix by **A**. Then instead of equation (3) we get another equation:

$$\boldsymbol{Ac} = \boldsymbol{\eta} \qquad (4)$$

Let's call this matrix **A** and this right-hand side *selective*.

Let two models be defined as follows:

1. *Model 1 (complete)*, where the *complete* matrix and the *complete* right-hand side are used;
2. *Model 2 (selective),* where the *selective* matrix and the *selective* right-hand side are used*;*

In both cases the matrices are ill-conditioned.

Regularization of the problem and the search for a quasi-solution is carried out by restricting to a subspace that is the linear hull of the *r* first right-hand singular vectors.

Singular Value Decomposition of the matrix **A** has been made and its singular system $\{\boldsymbol{v_i}, \boldsymbol{u_i}, s_i\}$ was defined. These are two orthonormal systems in the space of vectors $\{\boldsymbol{c}\}$ and in the space of right-hand side $\boldsymbol{\eta_0}$ In this case, vector $s_i\, \boldsymbol{u_i}$ will be called the *mode* generated by the singular vector $\boldsymbol{v_i}$

$$\mathbf{A}\, \boldsymbol{v_i} = s_i\, \boldsymbol{u_i}\,, \quad i = 1, \ldots, M \times N, \qquad (5)$$

Since singular values decrease rapidly as their indices increase, the number *r* must necessarily be bounded.

The quasi-solution obtained is a projection of the exact solution onto a linear hull of the *r* first right-hand singular vectors corresponding to the largest singular values of the matrix above:

$$\varphi^{[r]}(x, y) = \sum_{i=1}^{r} \alpha_i\, \Phi_i(x,\, y) = \sum_{i=1}^{r} \alpha_i \sum_{m=1}^{M} \sum_{n=1}^{N} \beta_{mn}^{i} \varphi_{mn}(x,\, y), \qquad (6)$$

where $\alpha_i = \frac{(\boldsymbol{\eta_0} \circ \mathbf{u_i})}{s_i}$; $\Phi_i(x,\, y) = \sum_{m=1}^{M} \sum_{n=1}^{N} \beta_{mn}^{i} \varphi_{mn}(x,\, y)$; $\boldsymbol{v_i} = (\beta_{11}^{i}, \beta_{12}^{i}, \ldots, \beta_{MN}^{i})$.

To obtain synthetic marigrams at locations of all sensors, it is necessary to take advantage of the fact that the responses to each spatial harmonic are already recorded in the columns of the complete matrix $\mathbf{A_0}$.

The vector $\boldsymbol{c} = \sum_{i=1}^{M \cdot N} \alpha_i\, \boldsymbol{v_i}$ contains the coefficients of the spatial harmonics of the source, so it is sufficient to sum the columns of the complete matrix $\mathbf{A_0}$ with these coefficients. The resulting vector will contain synthetic marigrams at locations of all sensors (or other points of interest).

We emphasize that when solving the direct problem, we always calculate the complete matrix $\mathbf{A_0}$. From this, we can then form any selective matrix. Synthetic marigrams can then be obtained both at the selected sensors and at the forecast points. There is no need to re-solve the direct problem.

Naturally, as the value of *r* increases, the information content of the resulting r-solution increases, but its stability deteriorates. The value of *r* depends on the rate of decreasing a singular spectrum of the matrix $\mathbf{A_0}$ which is tightly bonded with the tsunami sensors location, and in turn, should be considered as one of the main parameters of the efficiency of the inversion. By varying the value of r, one can control the instability in the solution. The relationship between the parameters r, N, M was investigated in (Voronina et al., 2019). The proposed approach, in which the solution is constructed based on the analysis of the operator properties determined by the selected observation system and the actual bathymetry, allows one to obtain the most reliable reconstruction result for the given conditions.

4 Selecting parameter *r*

As mentioned above, truncated singular value decomposition is a key element of the proposed method, so the value of the parameter *r* has a significant impact on the inversion result. The value of *r* is determined by taking into account the specific energy transferred by each mode.

The specific energy per unit fluid mass is proportional to the sum of the squared deviations of the time series (for the observed marigrams or for each mode). Each mode contains marigrams recorded sequentially by all

sensors. A sharp decrease in singular values as their indices increase indicates that only the first modes, corresponding to the first singular values, are significant for transmitting seismological information and energy.

As noted above, the left singular vectors $\{\boldsymbol{u_i}\}$, $i = 1, \ldots, N \times M$ are orthonormal, so the projection of vector $\boldsymbol{\eta_0}$ onto the subspace is vector $\boldsymbol{\eta_0^{[r]}} = \sum_{i=1}^{i=M\times N} \gamma_i \boldsymbol{u_i}$, where $\gamma_i = (\boldsymbol{\eta_0} \cdot \boldsymbol{u_i})$. The value of γ_i characterizes the share of energy transferred by the *i*-th mode to all sensors noted by E_i. These parameters are determined by the relations: $E_i = \gamma_i^2 / \|\boldsymbol{\eta}_0\|^2$; $i = 1, \ldots, N \times M$. The share of the specific energy corresponding to the *i*-th mode in the k-th sensor w. r. t. total energy in all sensors is determined by the formula $E_{ik} = \gamma_i^2 \cdot \sum_{j=N_t(k-1)+1}^{j=N_t k} u_{ij}^2 / \|\boldsymbol{\eta}_0\|^2$, where u_{ij} is the j-th component of the i-th left-hand singular vector, η_{0j} is the j-th component of the vector $\boldsymbol{\eta}_0$, the indices corresponding to the k-th sensor are from the interval $[N_t \cdot (k-1) + 1, N_t \cdot k]$. N_t is the number of time samples in each sensor's marigram.

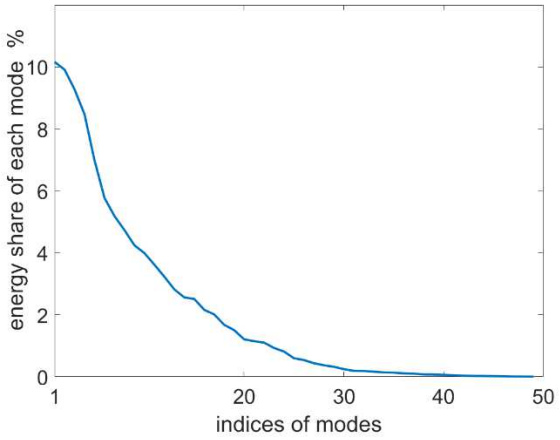


Fig. 2 Distribution (in percentage) of the energy transferred by each mode; the mode indices are on the horizontal axis

Figure 2 shows the distribution of specific energy over all modes as the ratio of the relative specific energy of the i-th mode. It is clear that the total share of the first 30 modes exceeds 80% of the total specific energy. In this case, a value of $r \leq 30$ can be chosen. Furthermore, the number of spatial harmonics should be determined using the method described in Voronina et al., (2019). Thus, analyzing the energy distribution of the modes (Fig. 2) provides immediate insight into what is a reasonable value of the parameter *r* to select for the inversion.

5 Selection of the Most Informative Sensors of the Observation Network

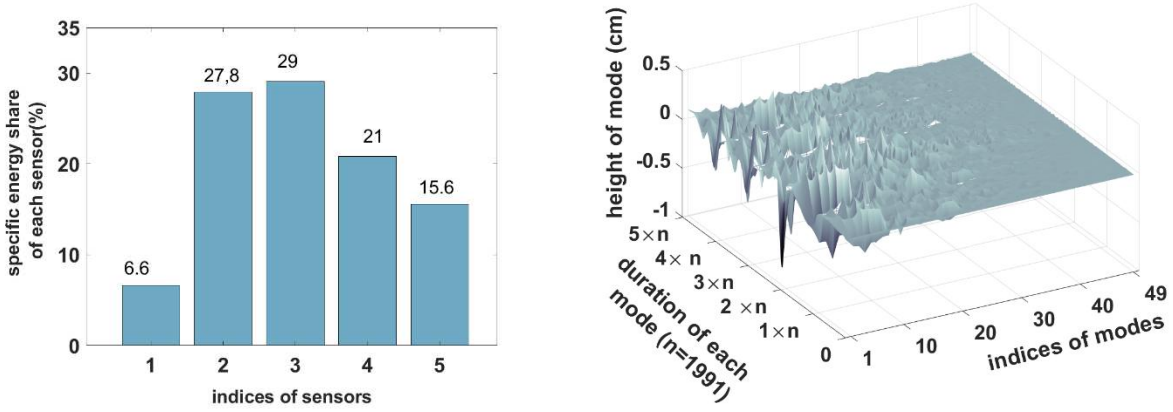
Further development of tsunami warning systems requires creating an effective observation system. A number of deep-sea tsunami sensor networks exist, such as the DART, DONET, and GPS buoy systems, which produce tsunami data in real time. Sea level records are typically highly noisy, so for reliable inversion results, the information content of the data, rather than their quantity, is crucial. The optimal spatial arrangement of tsunami sensors for use in the inversion of recorded tsunami waveforms has been discussed, for example, in (Mulia et al., 2017; Lee et al., 2019; Meza et al., 2018).

Already in model cases, it was revealed (Voronina et al., 2015) that the most informative direction coincides with the direction of the greatest variability of the model source. Moreover, these directions coincide with the direction of greatest energy transfer, since the maximum amplitudes are recorded in this direction. In previous studies (Voronina & Voronin, 2021,2023) dealing with real tsunamis (e.g., the Solomon Islands on February 6, 2013, Illapel on September 16, 2015, and Shikotan on October 5, 1994), the information content of observation systems was assessed based on an analysis of the distribution of specific wave energy among sensor locations (DART buoys). A general methodology for selecting the most informative sensor locations has been proposed in (Voronina & Voronin, 2025).

In this study, the same algorithm was used to find the optimal spatial distribution of DART buoys. The accumulation of specific energy at each sensor location is shown in Fig. 3a.

As can be seen in Fig. 3a, the modes arriving at DART buoys with identifiers 2, 3, and 4 have the largest amplitudes, indicating that they are of great importance for information acquisition and energy transfer. Fig. 3b shows a visual interpretation of 49 modes in 3D format for *Model 1* with parameters: $M = 7$, $N = 7$, $P = 5$, $dt = 2$ s, and $N_t = 1991$.

Based on the numerical experiments conducted, the following conclusion can be drawn: the most informative observation system is one whose data correspond to at least two-thirds of the total specific energy. We compared the results obtained from the complete system and from the selective system. In this case, we are dealing with a selective system consisting of DART buoys 21419, 21416, and 21415. The data recorded by these DART buoys are considered the most informative for the inversion procedure.



а) б)

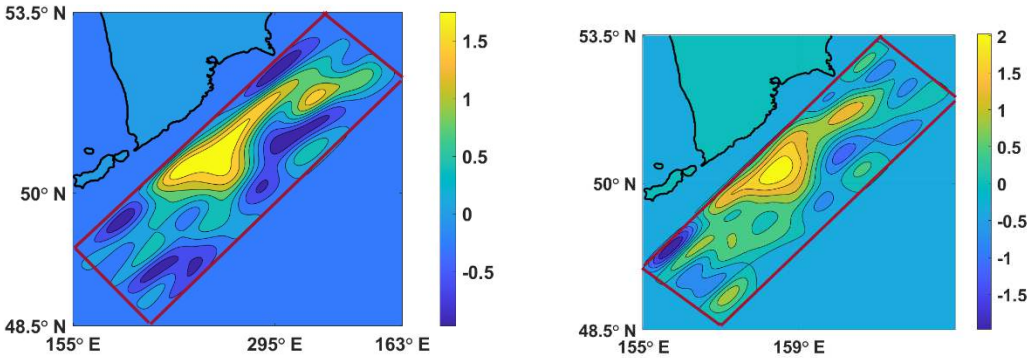
Fig. 3 a) Distribution diagram of specific energy (in percentage) at the locations of all sensors used: sensor indices are on the horizontal axis; specific energy (in percentage) is plotted along the vertical axis. b) 49 spatial modes in 3D format for *Model 1*: the duration of each mode is 5 × 1991 × 2 seconds; mode indices and duration of each mode are on the horizontal axes, respectively; heights of modes are on the vertical axis (in cm)

6 Results

The proposed method for reconstructing the tsunami source was applied to real tsunamis: the Solomon Islands Tsunami on February 6, 2013, and the Chilean Illapel Tsunami of September 16, 2015 (Voronina & Voronin, 2021,2023). The method of selecting the data and the inversion parameters was tested through numerical modeling of the above tsunamis. In the case under consideration, the experiments were carried out with data from the set of DART buoys marked by circles and enumerated clockwise in Fig. 1.

Model 1 (complete) was used with the following set of parameters: M = 7, N = 7; the total number of tsunami sensors P = 5; the matrix A: (49 × 9955); 1-arc-minute rectangular grid (2701 × 1801) in the entire simulation area; time sampled at 2 s intervals (P × N_t = 5 × 1991); bathymetry according to GEBCO_09 (http://www.gebco.net).

Model 2 (selective) was used with the following set of parameters: M = 7, N = 7; the matrix A: (49 × 5973); 1-arc-minute rectangular grid (2701 × 1801) in the entire simulation area; time sampled at 2 s intervals (P × N_t = 3 × 1991); the number of tsunami sensors P = 3; with records from DART buoys 2-21419, 3-21416, and 4-21415.



(a) (b)

Fig. 4 Tsunami initial displacement reconstructed by tsunami waveform inversion in the target domain: a) by *Model 1 (complete*): φ_{max} = 2.09, φ_{min} = −0.98, r = 37; b) *by Model 2* (selective) with records from DART buoys 2-21419, 3-21416, and 4=21415: φ_{max} = 2.42, φ_{min} = −1.97, r = 33. The color bar is in meters

Figure 4b shows the tsunami source reconstructed using the most informative data, which naturally reduces the overall percentage of noise in the data and increases the useful information, thereby reducing computational and time costs and improving the reliability of the inversion. Moreover, an additional advantage of using the most informative data is that, without recalculating wave propagation from the reconstructed source, one can obtain wave heights at locations where observations were not conducted but which were included in the calculation of the matrix A_0 in Eq. (3). Focusing on the calculation of amplitudes of incoming waves at locations where there are no observations, we applied the proposed approach to the Kamchatka Tsunami on July 29, 2025.

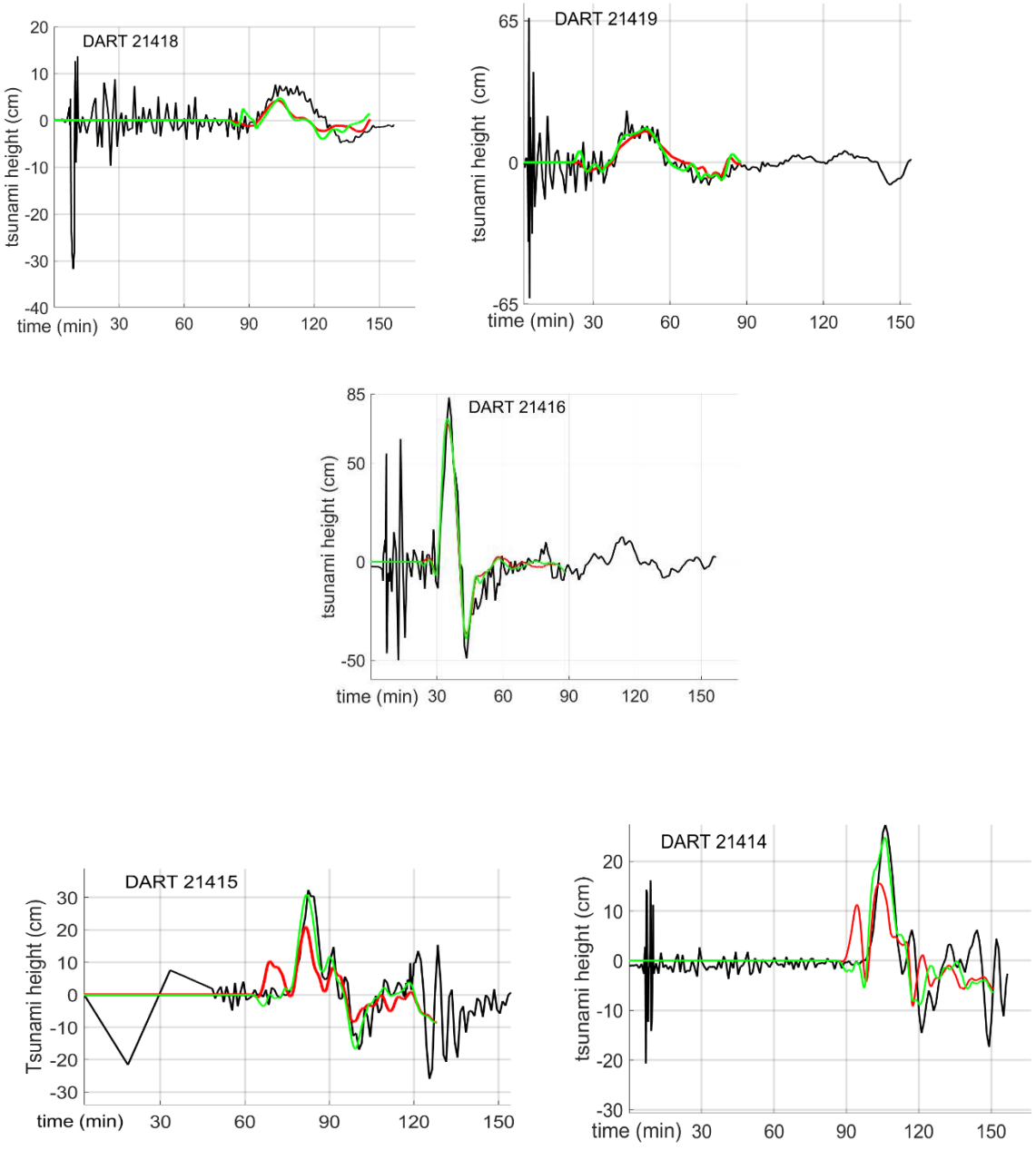


Fig. 5 Time-series of tsunami heights for five DART buoys 21418, 21419, 21416, 21415, 21414. The black curves show the observational data, the red and the green curves are corresponded to the inversion results obtained in the frame of the *Model 1* and the *Model 2*, respectively. DART buoy names are presented at the top of each panel. Time after Earthquake (min) is on the horizontal axis

In Figure 5 the recovered marigrams at the locations of all sensors, based on the coefficients produced in the inversion are presented. Station locations are shown in Fig.1. The green curves denote the calculated tsunami waveforms obtained from the selective system (*Model 2*) that is based on *the most informative data recorded by DART buoys 21419, 21416, 21415*; locations of DART buoys 1- 21418 and 5- 21414 act as forecast points. The red lines denote the inverted marigrams obtained using the complete system (*Model 1*). Adding significantly less

informative data from buoys 1-21418 and 5-21414 to the inversion reduces the accuracy of the reconstruction of the tsunami height.

It should be emphasized that only the most informative data allows us to reconstruct the tsunami height at predetermined locations where observation data are lacking. Otherwise, a reliable forecast is impossible.

We compared our results with those obtained using other approaches (e.g., at NOAA / PMEL / Center for Tsunami Research https://nctr.pmel.noaa.gov/kamchatka20250729/; Fujii & Satake 2026; Benz, 2025). Figure 6 shows the tsunami waveforms recorded by DART buoys 21419, 21416, and 21415 (black lines) alongside those obtained using wavefield modeling based on the reconstructed sources: the red lines correspond to the source model provided by the USGS (as of August, 7, 2025), and the light green lines correspond to the source reconstructed using

Model 2 (based the most informative data). The calculations of the forward problem with the above two recovered sources were performed by Beisel S. A. and Gusev O. I. (Federal Research Center for Information and Computational Technologies) using the MGC program (Chubarov et al., 2008, Shokin et al., 2008). The analysis of the obtained results allowed us to affirm that the tsunami source reconstructed by the method proposed corresponds well to the expected physical characteristics.

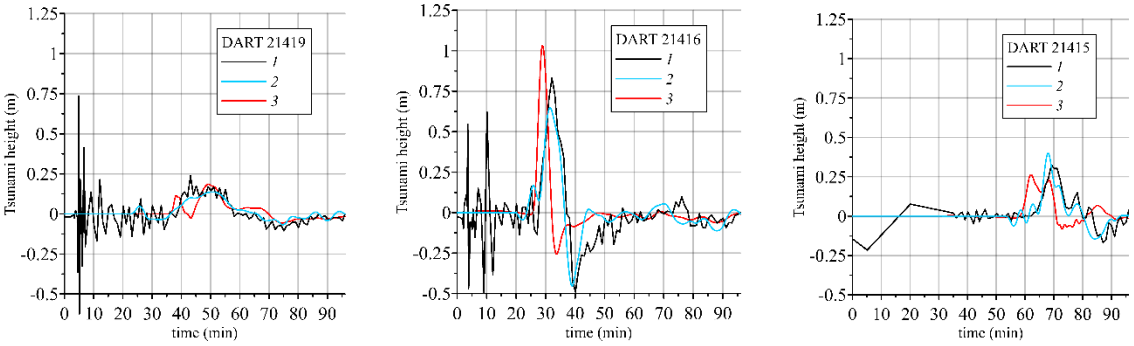


Fig. 6 Comparison of observed (black) and inverted waveforms at DART buoys 21419, 21416, and 21415. The red waveforms were obtained using the USGS source model calculated on August 7, 2025, while the green waveforms were reconstructed using the source shown in Fig. 4b. DART buoy names are presented at the top of each panel

This independent test with the reconstructed *Model 2* source confirms the validity of the obtained result. For Tsunami Warning Systems, computation speed is critical to ensuring timely forecasts. Computing the matrix $\mathbf{A_0}$ is the most time-consuming step. However, each column of matrix $\mathbf{A_0}$ can be calculated independently, the proposed algorithm enables parallel computations. This provides a speedup of up to M×N on M×N cores compared to a sequential implementation. The presented results were obtained using a parallel program running on a 64-core processor.

7 Conclusion

We applied the truncated singular value decomposition (SVD) method to reconstruct the source of the Tsunami that occurred on July 29 (30), 2025, in Kamchatka Peninsula area. Recordings from five DART buoys: 21418, 21419, 21416, 21415, 21414 were selected for inversion.

Based on numerical calculations, we concluded that the proposed method allows one to obtain tsunami amplitudes at locations with missing observations without solving the forward problem from the reconstructed tsunami source. Estimating the specific energy accumulation provides to select the most informative sensor locations. Using data obtained from the most informative sensors (21415, 21416, 21419) improves the quality of the source reconstruction and ensures better agreement between the synthetic and observed marigrams. Comparison of the obtained results with other studies confirmed the effectiveness of the proposed approach.

References

1.An, C., Liu, Philip L-F., and Meng,L. (2018). A sensitivity analysis of tsunami inversions on the number of stations. *Geophys. J. Int. Seismology*. 214, 1313–1323 doi: 10.1093/gji/ggy212

2.An, C., (2021). Tsunamis and tsunami warning: Recent progress and future prospects. *Science China Earth Sciences.* 64(2). DOI: 10.1007/s11430-020-9672-7

3. Baba, T., Takahashi, N., Kaneda, Y., Ando, K., Matsuoka, D., & Kato, T. (2015). Parallel Implementation of Dispersive Tsunami Wave Modeling with a Nesting Algorithm for the 2011 Tohoku Tsunami. *Pure and Applied Geophysics*, 172(12), 3455–3472. https://doi.org/10.1007/s00024-015-1049-2

4. Benz, H., Herman, M. Furlong, K., Jones, E., Schmitt, R., Yeck, W., and Barnhart, W. (2025). The 29 July 2025, M 8.8 Kamchatka Earthquake, U.S. Geological Survey StoryMap, https://earthquake.usgs.gov/storymap/index-kamchatka2025.html

5. Cheverda, V. A., & Kostin, V. I. (2010). r-pseudoinverse for compact operator. Siberian Electronic Mathematical Reports, Proceedings of the First International Youth Conference-School "Theory and Numerical Methods for Solving Inverse and Ill-Posed Problems". Part I. *Siberian Electronic Mathematical Reports*. 258–282. https://www.mathnet.ru/rus/semr287

6. Chubarov LB, Babailov VV, Beisel SA (2011.) Program for calculating parameters of seismogenetic tsunami waves MGC. *State Registration Certificate of Computer Program No. 2011614598.*

7. Fujii, Y., & Satake, K. (2026). The slip distributions of the 1952 and 2025 Kamchatka earthquakes from tsunami waveforms recorded around the Pacific Ocean. *Geophysical Research Letters*, 53, e2025GL120682. https://doi.org/10.1029/2025GL120682

8. Hossen, M. J., Gusman, A., Satake, K., & Cummins, P. R. (2018). An Adjoint Sensitivity Method Applied to Time Reverse Imaging of Tsunami Source for the 2009 Samoa Earthquake. *Geophysical Research Letters*, 45(2), 627–636. https://doi.org/10.1002/2017GL076031

9. National Oceanic and Atmospheric Administration. DART Data: 20250729_kamchatka. https://www.ngdc.noaa.gov/hazard/data/DART/20250729_kamchatka/

10. Lee, E., Jung, T., Kim, J.-C., & Shin, S. (2019). A Study of the Optimal Deployment of Tsunami Observation Instruments in Korea. *Journal of Ocean Engineering and Technology*, 33 (6), 607–614. https://doi.org/10.26748/KSOE.2019.100

11. Romano, F., Piatanesi, A., Lorito, S., Tolomei, C., Atzori, S., & Murphy, S. (2016). Optimal time alignment of tide-gauge tsunami waveforms in nonlinear inversions: Application to the 2015 Illapel (Chile) earthquake. *Geophysical Research Letters*, *43*(21). https://doi.org/10.1002/2016GL071310

12. Meza, J., Catalán, P. A., & Tsushima, H. (2018). A Methodology for Optimal Designing of Monitoring Sensor Networks for Tsunami Inversion. *Natural Hazards and Earth System Sciences Discussions.* https://doi.org/10.5194/nhess-2018-269

13. Mulia, I. E., & Asano, T. (2016). Initial tsunami source estimation by inversion with an intelligent selection of model parameters and time delays. *Journal of Geophysical Research: Oceans.* 121(1):441–456. DOI: 10.1002/2015JC010877

14. Mulia I E, Gusman A. R., and Satake K., (2017) Optimal design for placements of tsunami observing systems to accurately characterize the inducing earthquake. *Geophysical Research Letters*, 44 (24). DOI: 10.1002/2017GL075791

15. Mulia, I. E., Gusman, A. R., Hossen, M. J., & Satake, K. (2018). Adaptive tsunami source inversion using optimizations and the reciprocity principle. *Journal of Geophysical Research: Solid Earth*, 123(12), 10749–10760. https://doi.org/10.1029/2018JB016439

16. Mulia, I. E., Gusman, A. R., & Satake, K. (2020). Applying a deep learning algorithm to tsunami inundation database of megathrust earthquakes. *Journal of Geophysical Research: Solid Earth*, 125, 1–16, e2020JB019690. https://doi.org/10.1029/2020JB019690

17. NOAA / PMEL / Center for Tsunami Research (2025). Kamchatka Tsunami, July 29, 2025 Main Event Page. Retrieved from https://nctr.pmel.noaa.gov/kamchatka20250729/

18. Okal, E. A., & Synolakis, C. E. (2004). Source discriminants for near-field tsunamis. *Geophysical Journal International*, 158(3), 899–912. https://doi.org/10.1111/j.1365-246X.2004.02347.x

19. Percival, D. B., Denbo, D. W., Eble, M. C., Gica, E., Mofjeld, H. O., Spillane, M. C., Tang, L., & Titov, V. V. (2011). Extraction of tsunami source coefficients via inversion of DART buoy data. *Natural Hazards and Earth System Sciences*, 58, 567–590. https://doi.org/10.1007/s11069-010-9688-1

20. Piatanesi, A., Tinti, S., & Pagnoni, G. (2001). Tsunami waveform inversion by numerical finite-elements Green's functions. *Natural Hazards and Earth System Sciences*, 1, 187–194. https://doi.org/10.5194/nhess-1-187-200 1

21. Pires, C., & Miranda, P. M. A. (2001). Tsunami waveform inversion by adjoint methods. *Journal of Geophysical Research: Oceans*, 106(C9), 19773–19796. https://doi.org/10.1029/2000JC000334

22. Satake, K. (1987). Inversion of tsunami waveforms for the estimation of a fault heterogeneity: method and numerical experiments. *Journal of Physics of the Earth*, 35, 241–254. https://doi.org/10.4294/jpe1952.35.241

23. Satake, K. (1995). Linear and nonlinear computations of the 1992 Nicaragua earthquake tsunami. *Pure and Applied Geophysics,* 144(3), 455–470. https://doi.org/10.1007/BF00874378

24.Shokin, Y.I. et al. (2008). Mathematical Modeling in Application to Regional Tsunami Warning Systems Operations. In: Krause, E., Shokin, Y.I., Resch, M., Shokina, N. (eds) Computational Science and High Performance Computing III. Notes on Numerical Fluid Mechanics and Multidisciplinary Design, vol 101. Springer, Berlin, Heidelberg. https://doi.org/10.1007/978-3-540-69010-8_6

25. Song, T., Pang, C., Hou, B., Xu, G., Xue, J., Sun, H., & Meng, F. (2023). A review of artificial intelligence in marine science. *Frontiers in Earth Science*, 11, 1090185. https://doi.org/10.3389/feart.2023.1090185

26. Takagawa, T., Chida, Y., Fujik, T., & Kawaguchi, K. (2025). High-resolution source inversion of 2024 Noto Peninsula earthquake tsunami with modeling error corrections. *Scientific Reports*, 15, 24889. https://doi.org/10.1038/s41598-025-08978-0

27. Voronin, V. V., Voronina, T. A., & Tcheverda, V. A. (2015). Inversion method for initial tsunami waveform reconstruction. *Natural Hazards and Earth System Sciences*, 15 (6), 1251–1263. https://doi.org/10.5194/nhess-15-1251-2015

28. Voronina, T. A. (2011). Reconstruction of Initial Tsunami Waveforms by a Truncated SVD Method. *Journal of Inverse and Ill-Posed Problems*, 19(4-5), 615–629. https://doi.org/10.1515/jiip.2011.058

29. Voronina, T. A. (2016). Recovering a Tsunami Source and Designing an Observational System Based on an r-Solution Method. *Numerical Analysis and Applications*, 9(4), 267–276. https://doi.org/10.1134/S1995423916040017

30. Voronina, T. A., & Romanenko, A. A. (2016). The New Method of Tsunami Source Reconstruction With r-Solution Inversion Method. *Pure and Applied Geophysics*, 173, 4089–4099. https://doi.org/10.1007/s00024-016-1286-z

31. Voronina, T. A., Voronin, V. V., & Cheverda, V. A. (2019). The 2015 Illapel Tsunami Source Recovery by Inversion of DART Tsunami Waveforms Using the R-Solution Method. *Pure and Applied Geophysics,* 176(7), 2985–2993. https://doi.org/10.1007/s00024-019-02100-y

32. Voronina, T. A., & Voronin, V. V. (2021). A Study of Implementation Features of the r-Solution Method for Tsunami Source Recovery in the Case of the Illapel Tsunami 2015: Implementation Features of the r-Solution Method. *Pure and Applied Geophysics*, 178(12), 4853–4863. https://doi.org/10.1007/s00024-021-02843-7

33. Voronina, T. A., & Voronin, V. V. (2023). Data selection method for restoring a tsunami source form. *Geosystems of Transsition Zone*, 7(3), 292–303. https://doi.org/10.30730/gtrz.2023.7.3.292-303

34. Voronina, T. A., & Voronin, V. V. (2025). On the assessment of the efficiency of deep-sea monitoring sensors for a tsunami warning system. *Marine Geophysical Researches,* 46(2). https://doi.org/10.1007/s11001-025-09577-4

35. Wang, Y., Maeda, T., Satake, K., Heidarzadeh, M., Su, H., Sheehan, A. F., & Gusman, A. R. (2019). Tsunami Data Assimilation Without a Dense Observation Network. *Geophysical Research Letters*, 46(4), 2045–2053. https://doi.org/10.1029/2018GL080930

Author information

Authors and Affiliations

Voronina, Tatyana A. (https://orcid.org/0000-0002-3566-6203), Candidate of Sciences (Physics and Mathematics), Senior Researcher, Tsunami Laboratory, Institute of Computational Mathematics and Mathematical Geophysics of the Siberian Branch of RAS, Novosibirsk, tanvor@bk.ru

Voronin, Vladislav V. (https://orcid.org/0000-0002-1727-1873), Candidate of Sciences (Physics and Mathematics), Associate Professor, Higher Mathematics Chair, Department of mathematics and mechanics, Novosibirsk State University, Novosibirsk, vladvor48@bk.ru

Gorodnichev, Maxim A. (https://orcid.org/0000-0001-6580-0082), MSc in applied mathematics and computer science, Researcher, Laboratory of Parallel Program Synthesis, Institute of Computational Mathematics and Mathematical Geophysics of the Siberian Branch of RAS; Lecturer, Novosibirsk State University, Novosibirsk State Technical University, maxim@ssd.sscc.ru

Competing interests.

The authors declare no competing interests

Declaration of interests

The authors declare that they have no known competing financial interests or personal relationships that could have appeared to influence the work reported in this paper.

Contributions

VTA: Conceptualization, Methodology, Software, Writing - Original Draft, Visualization.
VVV: Methodology, Investigation**,** Validation.
GMA: Parallel programming, program optimization, computational experiments.

The first draft of the manuscript was written by Voronina Tatyana A. and all authors commented on previous versions of the manuscript. All authors read and approved the final manuscript.

Corresponding author
Correspondence to Voronina, Tatyana A.